Mineralogical Magazine, February 2010, Vol. 74(1), pp. 39–53

Description and crystal structure of a new mineral, edwardsite, $Cu_3Cd_2(SO_4)_2(OH)_6 \cdot 4H_2O$, from Broken Hill, New South Wales, Australia

P. ELLIOTT[1,2,*], J. BRUGGER[1,2] AND T. CARADOC-DAVIES[3]

[1] School of Earth and Environmental Sciences, The University of Adelaide, Adelaide, South Australia 5005, Australia
[2] South Australian Museum, North Terrace, Adelaide, South Australia 5000, Australia
[3] Australian Synchrotron, 800 Blackburn Road, Clayton, Victoria 3168, Australia

[*Received 11 December 2009; Accepted 31 January 2010*]

ABSTRACT

Edwardsite, $Cu_3Cd_2(SO_4)_2(OH)_6 \cdot 4H_2O$, is a new mineral from the Block 14 Opencut, Broken Hill, New South Wales, Australia. It occurs as druses of tabular and bladed crystals up to 0.06 mm in size, associated with niedermayrite and christelite. Edwardsite is pale blue, transparent with vitreous lustre and has excellent cleavage parallel to {100}. Density was not measured but the calculated density, from the empirical formula, is 3.53 g cm^{-3} and the Mohs hardness is ~3. Optically, it is biaxial negative with $\alpha \sim 1.74$, $\beta = 1.762(4)$, $\gamma \sim 1.77$ and $2V_{calc.} \sim +62°$. The optical orientation is X = *b*, Y ~ *a*, Z ~ *c*. Electron microprobe analysis gave (wt.%): CdO 32.43, CuO 28.06, ZnO 2.26, FeO 0.08, SO_3 20.35, $H_2O_{calc.}$ (from crystal-structure analysis) 14.14, totalling 99.32. The empirical formula, calculated on the basis of 18 oxygen atoms is $Cu_{2.77}Cd_{1.98}Zn_{0.22}Fe_{0.01}(SO_4)_{2.00}(OH)_{5.95} \cdot 4.06H_2O$. Edwardsite is monoclinic, space group $P2_1/c$, with a = 10.863(2) Å, b = 13.129(3) Å, c = 11.169(2) Å, β = 113.04(3)°, V = 1465.9(5) Å^3 (single-crystal data) and Z = 4. The eight strongest lines in the powder diffraction pattern are [d (Å), (I/I_0), (hkl)]: 9.991, (90), (100); 5.001, (90), (200, $21\bar{1}$); 4.591, (45), ($20\bar{2}$); 3.332, (60), (300, 032); 3.005, (30), ($0\bar{2}3$); 2.824, (40), ($\bar{1}\bar{4}2$); 2.769, (55), ($20\bar{4}$, 042, $10\bar{4}$); 2.670, (45), ($2\bar{4}\bar{2}$). The crystal structure was determined by direct methods and refined to $R1$ = 3.21% using 1904 observed reflections with $F_o > 4\sigma(F_o)$ collected using synchrotron X-ray radiation (λ = 0.773418 Å). The structure is based on infinite sheets of edge-sharing $Cu\phi_6$ (ϕ: O^{2-}, OH) octahedra and $Cd\phi_7$ (ϕ: O^{2-}, H_2O) polyhedra parallel to (100). The sheets are decorated on both sides by corner-sharing (SO_4) tetrahedra, which also corner-link to isolated $Cd\phi_6$ octahedra, thus connecting adjacent sheets. Moderate-strong to weak hydrogen bonding provides additional linkage between sheets.

KEYWORDS: edwardsite, new mineral species, crystal structure, Cd oxysalt, sulphate, Broken Hill, New South Wales.

Introduction

IN about 2001, a specimen of an unidentified sulphate mineral forming druses of pale blue crystals was collected on ore stockpiles that had been mined from the Block 14 Opencut, Broken Hill and dumped at the Pinnacles Mine, 15 km southwest of Broken Hill. Subsequently, in 2006, the specimen was submitted to one of the authors (P.E.) for identification. Preliminary chemical analyses and X-ray diffraction showed that the mineral was a Cu-Cd sulphate with a powder X-ray diffraction pattern that could not be matched to any known mineral or synthetic compound. Initial single-crystal studies were not successful due to the small size of the crystals and a complete characterization of the mineral has been possible only after collection of single-

---

* E-mail: peter.elliott@adelaide.edu.au
DOI: 10.1180/minmag.2010.074.1.39

crystal X-ray data using sychrotron radiation. Edwardsite represents only the third known Cd-bearing sulphate mineral after IMA2002-034, $CdSO_4·4H_2O$ (IMA Commission on New Minerals, Nomenclature and Classification website at http://pubsites.uws.edu.au/ima-cnmnc/) and niedermayrite $Cu_4Cd(SO_4)_2(OH)_6·4H_2O$, (Giester *et al.*, 1998). A further natural Cd sulphate, $CdSO_4·H_2O$, is known from Radvanice near Trutnov, Czech Republic (Bregeault and Herpin, 1970; Sejkora and Kotrlý, 1998), but remains to be described as a new mineral species. The name edwardsite is for Dr Austin Burton Edwards (1909–1960), mineralogist and petrologist from 1934–1960 in the Mineragraphic Section of the Council for Scientific and Industrial Research (CSIR), later the Commonwealth Scientific and Industrial Research Organisation (CSIRO), Melbourne, Australia, and is in recognition of his contribution to the earth sciences, in particular, studies of the geology, geochemistry and mineralogy of Australian ore deposits, which included the publication of 18 papers on Broken Hill geology and mineralogy. The name edwardsite was previously given to a Ce-Zr phosphate mineral from Norwich, Connecticut, USA by Shepard (1837). The mineral was later discredited and shown to be monazite-Ce (Shepard, 1840). The new mineral and its name have been approved by the I.M.A. Commission on New Minerals, Nomenclature and Classification, (IMA 2009-048). The holotype specimen is deposited in the South Australian Museum, Adelaide, South Australia, (registration number G32703).

Occurrence

The Broken Hill Ag-Pb-Zn deposit is the largest Pb-Zn orebody in the world. It is Australia's most mineralogically diverse mineral deposit and has produced approximately 300 different mineral species, including 16 type-locality species (Birch, 1999). The deposit consists of six discrete, parallel and stratigraphically-controlled lenses of sulphide-rich rocks, comprising four Zn lodes and two Pb lodes within highly deformed siliclastic metasedimentary rocks of the Palaeoproterozoic Willyama Supergroup (Willis *et al.*, 1983; Stevens, 1998). Primary sulphides are rich in Pb, Zn, Ag, Mn and Cu with significant amounts of F, P, As, Sb, Co, Ni and Cd (Plimer, 1984) and each of the orebodies has a characteristic chemistry and mineralogy. The primary ores contain small concentrations of Cd, principally as an isomorphic replacement for Zn in sphalerite, the main Zn ore mineral (Edwards, 1955; Both, 1973). The Cd content shows significant differences between lenses, with the No. 3 lens, which was mined in the Block 14 Opencut, showing up to 3000 ppm Cd.

The Broken Hill oxidized zone has proved to be an important source of secondary Cd minerals. Edwardsite is the third new Cd-dominant mineral to be described from Broken Hill after birchite, $Cd_2Cu_2(PO_4)_2(SO_4)·5H_2O$, (Elliott *et al.*, 2008) and nyholmite, $Cd_3Zn_2(AsO_3OH)_2(AsO_4)_2·4H_2O$, (Elliott *et al.*, 2009). In addition, the secondary Cd minerals otavite, $CdCO_3$, goldquarryite, $CuCd_2Al_3(PO_4)_4F_2(H_2O)_{10}(H_2O)_2$, and niedermayrite, $Cu_4Cd(SO_4)_2(OH)_6·4H_2O$, have been identified from Broken Hill, as have cadmian varieties of conichalcite-duftite, sampleite-lavendulan-zdenekite (Giester *et al.*, 2007), christelite and serpierite.

Appearance, physical and optical properties

Edwardsite occurs as druses and aggregates of tabular to bladed crystals, of maximum length 0.06 mm (Fig. 1). The crystals are transparent, pale blue, with a vitreous lustre and white streak. The mineral is brittle, with an uneven fracture and an excellent cleavage on {100}. The crystals are flattened on {100} and often elongated along [010], with predominant crystal forms {100}, {001} and possibly {043}, with minor {010} plus other minor prisms and domes (Fig. 2). Edwardsite is not fluorescent under either long-

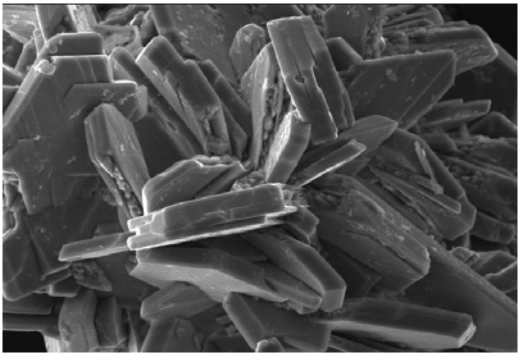

FIG. 1. SEM photomicrograph showing crystals of edwardsite. The crystals are flattened on (100) and elongated along [010] and show the principal forms {100} and {001}, with minor {010} and possibly {043}. The field of view is 80 μm across.

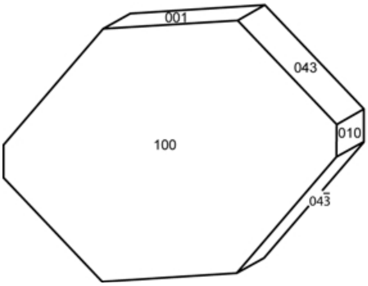

FIG. 2. Edwardsite crystal drawing showing the principal forms present; the tabular crystal is flattened on {100} and elongated along [010]. Crystal modelled with *SHAPE V7.1.2* (Shape Software, 2004).

or short-wave ultraviolet light. The crystals are too small to ascertain hardness, but the Mohs hardness is estimated to be ~3–3.5. The density could not be measured and the optical properties could not be characterized completely due to the tiny size of available crystals and scarcity of the mineral. The calculated density, on the basis of the empirical formula, is 3.53 g cm^{-3}. Crystals are biaxial (–) with α ~1.74, β = 1.762(4), γ ~1.77 (values obtained in white light using Cargille immersion liquids), and $2V_{calc.}$ ~ +62º. Optical orientation is X = *b*, Y ~ *a*, Z ~ *c*, with inclined extinction and crystals show negative elongation (i.e. they are length-fast). Edwardsite shows no pleochroism: X = Y = Z pale greyish-blue.

Chemical composition

A crystal aggregate of edwardsite was embedded in epoxy, polished, carbon-coated and analysed with a Cameca SX51 electron microprobe operated in wavelength-dispersive mode. Operating conditions were as follows: excitation voltage 15 kV, probe current 10 nA, a final beam diameter of 10 μm, peak count-times 20 s and background count-times 10 s. The results, as well as the standards used, are shown in Table 1. The mineral decomposes rapidly under the electron beam and the small size of the crystals presented difficulties in employing a defocused beam and as a result analytical totals were variable. Data were reduced using the method of Pouchou and Pichoir (1985). Elements present in minor amounts (<0.05 wt.% oxide) are Al, Ca, Mn, Pb and P. No other elements with atomic number ⩾9 were detected. Due to the very small amount of the mineral available, a direct water determination could not be carried out, but the presence of H_2O was confirmed by the crystal-structure solution and by infrared spectroscopy. The empirical formula, calculated on the basis of 18 oxygen atoms, is $Cu_{2.77}Cd_{1.98}Zn_{0.22}Fe_{0.01}(SO_4)_{2.00}(OH)_{5.95}\cdot4.06H_2O$. The simplified formula is $Cu_3Cd_2(SO_4)_2(OH)_6\cdot4H_2O$, which requires CuO 30.53 wt.%, CdO 32.85, SO_3 20.48, H_2O 16.14, totalling 100.00 wt.%.

Infrared spectroscopy

An infrared absorption spectrum of edwardsite was obtained using a Nicolet 5700 FTIR spectrometer equipped with a Nicolet Continuum IR microscope and a diamond-anvil cell. A crystal aggregate was crushed in the diamond cell and a spectrum recorded in the range 4000 to 650 cm^{-1} (Fig. 3). The spectrum shows a broad band due to O–H stretching from 3655–2810 cm^{-1} with a peak at 3488 cm^{-1} and a shoulder at 3345 cm^{-1}.

TABLE 1. Compositional data for edwardsite.

Constituent	Wt.%	Range	Stand. Dev.	Probe Standard
CuO	28.06	25.96–30.59	1.50	chalcopyrite
ZnO	2.26	0.86–2.65	0.55	sphalerite
CdO	32.43	30.72–34.02	1.33	Cd metal
FeO	0.08	0.00–0.17	0.06	almandine
SO_3	20.35	17.67–23.01	1.71	chalcopyrite
H_2O*	16.14			
Total	99.32			

Number of analyses = 10.
* Calculated from the ideal formula based on structure determination.
The empirical formula based on 18 oxygen atoms is: $Cu_{2.77},Cd_{1.98},Zn_{0.22},Fe_{0.01}(SO_4)_{2.00}(OH)_{5.95}\cdot4.06H_2O$

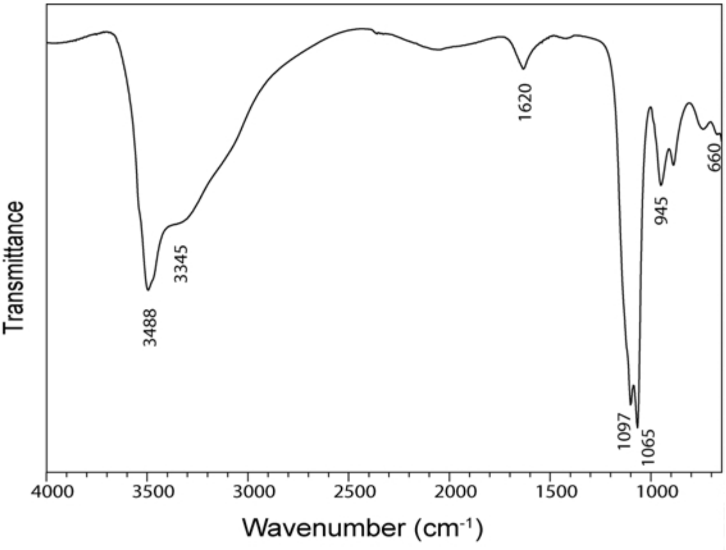

FIG. 3. FT-IR spectrum of powdered edwardsite.

The absorption band at 1620 cm^{-1} is due to H–O–H bending, indicating the presence of molecular water. A strong split band at 1097 and 1065 cm^{-1} is attributable to the SO^{4-} asymmetric stretch ν_3, a band at 945 cm^{-1} is attributable to the SO^{4-} symmetric stretch ν_1 and a weak band at 660 cm^{-1} is attributable to the SO^{4-} asymmetric bend ν_4. Based on the correlation curve established by Libowitzky (1999), values of the νOH vibrational frequencies indicate the presence of medium-strong to weak H bonds in the structure of edwardsite, with H···O distances of 1.67–2.56 Å (O···O distances of 2.61–3.10 Å), which compares to the observed H···O distances of 1.763–2.554 Å (O···O distances of 2.679–3.06 Å).

X-ray powder diffraction data

X-ray powder-diffraction data (Table 2) were obtained with a 100 mm Guinier-Hägg camera using Cr-$K\alpha$ radiation (λ = 2.28970 Å) and silicon (NBS SRM 640a) as an internal standard. Intensities were visually estimated and the calculated intensities were obtained from the structural model. The Guinier-Hägg film was scanned using an Epson film scanner, the powder-diffraction profile over the 2θ range 10 to 90° was extracted and the unit-cell parameters were refined using the Le Bail profile-fitting method (Le Bail *et al.*, 1988; Hunter, 1998) starting from the unit-cell parameters determined from single-crystal techniques. The unit-cell parameters refined from the powder data are a = 10.845(4) Å, b = 13.118(4) Å, c = 11.158(6) Å, β = 112.987(6)°, V = 1461.2(2) Å^3, which agree with those refined using single-crystal methods.

Structure determination

Single-crystal X-ray data collection

An initial attempt to collect single-crystal X-ray data was made using a Nonius KappaCCD diffractometer. However, 200 s exposures per frame-width did not yield more than 1 or 2 reflections on each frame. Therefore, X-ray intensity data were obtained at the Australian Synchrotron facility using a crystal of dimensions 0.033 mm × 0.025 mm × 0.008 mm. Data were collected using a ADSC Quantum 210r detector using monochromatic X-radiation λ = 0.773418 Å) by scanning in ϕ and ω with frame widths of 2° and 10 s spent counting per frame. The unit-cell dimensions, refined using least squares techniques, are a = 10.863(2) Å, b = 13.129(3) Å, c = 11.169(2) Å, β = 113.04(3)°. The measured intensities were corrected for Lorentz, polarization and absorption effects. A total of 16269 reflections were collected, of which 2258 were unique with 1904 classed as observed $F_o > 4\sigma(F_o)$. Details of data collection and structure refinement are listed in Table 3.

TABLE 2. X-ray powder diffraction data for edwardsite.

$I_{obs.}$	$d_{obs.}$	$I_{calc.}$	$d_{calc.}$	h	k	l
90	**9.991**	**83**	**9.997**	**1**	**0**	**0**
10	8.105	6	8.093	0	1	1
10	7.959	8	7.953	1	1	0
20	7.522	9	7.526	1	1	$\bar{1}$
20	6.564	7	6.565	0	2	0
10	5.538	2	5.536	1	0	$\bar{2}$
		7	5.514	1	1	1
15	5.489	13	5.487	1	2	0
5	5.149	12	5.139	0	0	2
90	**5.001**	**100**	**4.998**	**2**	**0**	**0**
		14	**4.996**	**2**	**1**	**$\bar{1}$**
20	4.800	9	4.786	0	1	2
20	4.673	6	4.671	2	1	0
45	**4.591**	**42**	**4.592**	**2**	**0**	**$\bar{2}$**
20	4.461	27	4.459	1	2	1
15	4.270	1	4.335	2	$\bar{1}$	$\bar{2}$
10	4.236	0	4.232	1	$\bar{2}$	$\bar{2}$
		4	4.047	0	2	2
15	3.805	1	3.809	1	1	2
		5	3.763	2	$\bar{2}$	$\bar{2}$
5	3.599	1	3.577	1	$\bar{1}$	$\bar{3}$
5	3.478	3	3.488	3	0	$\bar{2}$
20	3.423	12	3.424	2	$\bar{1}$	$\bar{3}$
15	3.377	15	3.372	2	2	1
		3	3.371	3	1	$\bar{2}$
60	3.332	26	3.332	3	0	0
		12	3.332	0	3	2
10	3.281	16	3.282	0	4	0
5	3.237	5	3.235	1	$\bar{2}$	$\bar{3}$
10	3.230	6	3.217	3	1	0
10	3.209	8	3.164	3	2	$\bar{1}$
		3	3.091	1	4	$\bar{1}$
20	3.005	1	3.037	0	2	$\bar{3}$
5	2.985	5	2.982	3	1	$\bar{3}$
5	2.948	1	2.945	1	3	2
5	2.890	5	2.888	1	4	1
5	2.853	7	2.841	1	1	3
40	**2.824**	**14**	**2.823**	**1**	**$\bar{4}$**	**$\bar{2}$**
		3	2.793	3	1	1
		3	2.785	3	3	$\bar{1}$
55	**2.769**	**6**	**2.768**	**2**	**0**	**$\bar{4}$**
		5	**2.766**	**0**	**4**	**2**
		20	**2.763**	**1**	**0**	**$\bar{4}$**
10		2	2.757	2	2	2
		6	2.727	3	3	$\bar{2}$
5	2.698	3	2.698	0	3	3
45	**2.670**	**25**	**2.670**	**2**	**$\bar{4}$**	**$\bar{2}$**
		7	2.581	3	0	$\bar{4}$
15	2.578	20	2.570	0	0	4
5	2.536	2	2.533	3	$\bar{1}$	$\bar{4}$
		5	2.532	1	4	2
5	2.501	7	2.502	4	1	$\bar{3}$
		5	2.496	2	3	2
5	2.459	0	2.461	1	$\bar{4}$	$\bar{3}$
		3	2.429	3	4	$\bar{1}$
5	2.406	1	2.402	3	$\bar{2}$	$\bar{4}$
20	2.389	13	2.390	3	4	$\bar{2}$
		3	2.325	2	5	0
10	2.289	12	2.283	1	0	4
5	2.275	3	2.280	2	5	$\bar{2}$
5	2.233	4	2.229	2	4	2
5	2.191	2	2.192	1	5	2
		4	2.188	0	6	0
5	2.161	3	2.160	1	1	$\bar{5}$
5	2.139	4	2.140	0	6	1
5	2.117	3	2.116	4	2	1
		3	2.114	1	$\bar{4}$	$\bar{4}$
5	2.085	8	2.086	4	4	$\bar{2}$
5	2.066	2	2.077	4	4	$\bar{1}$
5	2.028	1	2.029	3	$\bar{4}$	$\bar{4}$
5	2.006	2	2.005	2	$\bar{6}$	0
		4	2.003	5	0	$\bar{4}$
5	1.997	7	2.002	3	1	3
		4	1.999	4	1	$\bar{5}$
		6	1.990	2	0	4
		3	1.980	5	1	$\bar{4}$
5	1.973	1	1.977	5	1	0
		3	1.968	2	1	4
5	1.944	9	1.946	5	3	$\bar{2}$
		3	1.883	4	5	$\bar{2}$
		3	1.821	5	3	$\bar{4}$
5	1.812	3	1.812	2	3	4
		3	1.812	5	4	$\bar{2}$
5	1.792	3	1.793	4	3	2

Intensities estimated visually. $I_{calc.}$ calculated with program *LAZY PULVERIX* (Yvon *et al.*, 1977).

Structure solution and refinement

Scattering curves for neutral atoms were taken from the International Tables for Crystallography (Wilson, 1992). The *SHELX 97* programs (Sheldrick, 1997*a*,*b*) were used for the structure determination and refinement. Systematic absences and reflection statistics ($|E^2-1| = 0.964$) indicated the centrosymmetric space group $P2_1/c$. The structure was solved by direct methods and the resulting model contained the positions of all Cd, Cu and S cations. The positions of 18 O atoms were found on subsequent difference-Fourier maps

TABLE 3. Crystal data, data collection and refinement details.

Crystal data	
Formula	$Cu_3Cd_2(SO_4)_2(OH)_6 \cdot 4H_2O$
Space group	$P2_1/c$
a, b, c (Å)	10.863(2), 13.129(3), 11.169(2)
β (º)	113.04(3)
V (Å^3), Z	V = 1465.9(5), 4
F(000)	1484.0
μ (mm^{-1})	7.540
Crystal dimensions (mm)	0.033 × 0.025 × 0.008
Data collection	
Diffractometer	ADSC Quantum 210r
Temperature (K)	123
Wavelength	λ = 0.773418 Å
θ range (º)	9.56–23.53
Detector distance (mm)	83.97
Rotation axes	φ ω
Rotation width (º)	2.0
Total no. of frames	180
Collection time per frame (s)	10
h,k,l ranges	−12 → 12, −14 → 14, −12 → 11
Total reflections measured	16269
Data completeness (%)	88.9
Unique reflections	2258 (R_{int} = 0.0423)
Refinement	
Refinement on	F^2
$R1^*$ for $F_o > 4\sigma(F_o)$	3.21%
$wR2^\dagger$ for all F_o^2	8.31%
Reflections used $F_o > 4\sigma(F_o)$	1904
Number of parameters refined	274
Extinction factor	0.0019(5)
Δρmin, Δρmax (e/Å3)	2.236, $\bar{1}$.079
Goodness of Fit	1.078

* $R1 = \Sigma||F_o| - |F_c||/\Sigma|F_o|$

† $wR2 = \Sigma w(|F_o|^2 - |F_c|^2)^2/\Sigma w|F_o|^2)^{1/2}$; $w = 1/[\sigma^2(F^2_o) + (0.042\ P)^2 + 12.60\ P]$;
$P = [\{\max \text{ of } (0 \text{ or } F_0^2)\} + 2F_c^2]/3$

calculated by least-squares refinement and the refinement converged to an R index of 3.90% for a model with anisotropic-displacement parameters for all atoms (except H). The locations of 14 H atoms obtained from difference-Fourier maps, and their positional parameters were added to the refinement with a resulting final R index of 3.21%. The final atomic-positional parameters and anisotropic-displacement parameters are given in Table 4, selected interatomic distances and angles are given in Table 5 and the results of the bond-valence analysis (Brown and Altermatt, 1985; Brese and O'Keeffe, 1991; Brown, 1996) are given in Table 6.

Structure description

Cation coordination

The structure contains four symmetrically distinct Cu sites, each coordinated by four OH groups and two O^{2-} anions in a distorted octahedral arrangement, such that each octahedron contains four short (range: 1.947(4)–1.984(5) Å) Cu–O bond lengths to OH groups (Table 5) arranged at the vertices of a planar square, and two long bond lengths (range: 2.430(4)–2.838(5) Å) to apical O(2) and O(5) anions. Such (4 + 2) coordination is typical for Cu^{2+} oxysalts owing to the Jahn-Teller effect (Jahn and Teller, 1937; Burns and Hawthorne, 1996). Because of the similarity of

TABLE 4. Fractional atomic coordinates and displacement parameters (in Å^2) for edwardsite.

Atom	x	y	z	U_{eq}	U_{11}	U_{22}	U_{33}	U_{12}	U_{13}	U_{23}
Cd(1)	−0.00341(4)	0.56798(3)	0.31880(4)	0.0103(2)	0.0103(3)	0.0079(3)	0.0123(3)	0.00036(16)	0.0039(2)	−0.00009(16)
Cd(2)*	0.56339(5)	0.61959(3)	0.77299(5)	0.0117(3)	0.0201(4)	0.0057(4)	0.0105(4)	−0.00116(17)	0.0074(2)	−0.00215(17)
Cu(1)	0.52495(7)	0.74448(5)	1.01316(7)	0.0095(3)	0.0117(4)	0.0060(4)	0.0105(5)	−0.0010(3)	0.0041(3)	0.0003(3)
Cu(2)	0.5	0.5	1	0.0093(3)	0.0111(5)	0.0067(5)	0.0096(6)	−0.0014(4)	0.0036(4)	−0.0007(4)
Cu(3)	0.5	0.5	0.5	0.0095(3)	0.0115(5)	0.0065(5)	0.0103(6)	0.0007(4)	0.0042(4)	0.0013(4)
Cu(4)	0.49372(7)	0.37193(5)	0.74106(7)	0.0091(3)	0.0115(4)	0.0059(4)	0.0105(5)	−0.0003(3)	0.0050(3)	0.0005(3)
S(1)	0.18421(15)	0.38395(11)	0.49236(15)	0.0092(4)	0.0103(8)	0.0069(7)	0.0101(8)	0.0000(6)	0.0037(6)	0.0006(5)
S(2)	0.19454(15)	0.61158(11)	0.89026(15)	0.0095(4)	0.0101(8)	0.0077(7)	0.0115(8)	−0.0018(6)	0.0051(6)	−0.0007(5)
O(1)	0.1302(5)	0.2814(3)	0.4883(5)	0.0157(10)	0.021(2)	0.007(2)	0.020(3)	0.0017(18)	0.008(2)	−0.0021(18)
O(2)	0.3292(4)	0.3803(3)	0.5269(4)	0.0112(10)	0.010(2)	0.014(2)	0.007(2)	−0.0018(16)	0.0001(18)	0.0002(16)
O(3)	0.1550(4)	0.4483(3)	0.5877(4)	0.0118(9)	0.014(2)	0.009(2)	0.015(2)	−0.0018(17)	0.0083(19)	0.0016(17)
O(4)	0.1222(4)	0.4307(3)	0.3604(4)	0.0125(10)	0.017(2)	0.011(2)	0.010(2)	0.0044(17)	0.0054(18)	0.0050(17)
O(5)	0.3288(4)	0.6217(3)	0.9932(5)	0.0133(10)	0.012(2)	0.012(2)	0.015(3)	−0.0006(17)	0.0038(19)	−0.0011(16)
O(6)	0.1857(4)	0.6688(3)	0.7728(4)	0.0141(10)	0.017(2)	0.013(2)	0.012(2)	0.0029(18)	0.0056(18)	0.0006(18)
O(7)	0.0944(4)	0.6526(3)	0.9380(4)	0.0139(9)	0.018(2)	0.011(2)	0.015(2)	−0.0020(18)	0.0084(19)	−0.0003(18)
O(8)	0.1663(4)	0.5021(3)	0.8562(4)	0.0134(9)	0.013(2)	0.009(2)	0.016(2)	−0.0012(18)	0.0025(18)	0.0019(17)
OH(9)	0.6077(5)	0.6175(3)	0.9863(5)	0.0148(10)	0.013(2)	0.011(2)	0.020(3)	−0.0037(18)	0.005(2)	−0.0012(17)
OH(10)	0.6095(4)	0.7275(3)	1.2014(4)	0.0110(9)	0.011(2)	0.008(2)	0.012(2)	0.0000(17)	0.0023(18)	0.0032(17)
OH(11)	0.5573(4)	0.2527(3)	0.6770(4)	0.0126(10)	0.017(2)	0.009(2)	0.014(3)	0.0033(17)	0.0082(19)	0.0031(18)
OH(12)	0.4316(4)	0.4903(3)	0.8079(4)	0.0114(9)	0.012(2)	0.011(2)	0.013(2)	−0.0048(17)	0.0061(18)	−0.0031(17)
OH(13)	0.4426(4)	0.6310(3)	0.5499(4)	0.0110(9)	0.014(2)	0.007(2)	0.012(2)	0.0006(16)	0.0049(19)	0.0014(16)
OH(14)	0.4044(4)	0.5295(3)	0.3157(4)	0.0125(9)	0.013(2)	0.014(2)	0.012(2)	0.0012(18)	0.0070(18)	0.0011(18)
H_2O(15)	0.1335(5)	0.6248(3)	0.2090(5)	0.0175(10)	0.020(3)	0.016(2)	0.019(3)	−0.0002(19)	0.011(2)	−0.0026(18)
H_2O(16)	0.1566(4)	0.6507(3)	0.4978(5)	0.0138(9)	0.015(2)	0.009(2)	0.018(3)	0.0015(18)	0.0068(19)	0.0001(18)
H_2O(17)	−0.1000(5)	0.7201(3)	0.2504(5)	0.0173(10)	0.024(3)	0.008(2)	0.019(3)	0.0018(19)	0.007(2)	0.0016(19)
H_2O(18)	0.7994(5)	0.5979(4)	0.8606(5)	0.0247(11)	0.017(3)	0.023(3)	0.031(3)	−0.001(2)	0.006(2)	−0.004(2)
H(1)	0.700(5)	0.615(7)	1.011(10)	0.035(7)						
H(2)	0.698(5)	0.707(7)	1.226(9)	0.035(7)						
H(3)	0.644(6)	0.228(7)	0.700(10)	0.035(7)						
H(4)	0.336(5)	0.488(7)	0.771(9)	0.035(7)						
H(5)	0.353(5)	0.634(7)	0.534(10)	0.035(7)						
H(6)	0.321(6)	0.556(7)	0.302(10)	0.035(7)						
H(7)	0.143(9)	0.696(4)	0.206(8)	0.035(7)						
H(8)	0.116(10)	0.601(6)	0.125(6)	0.035(7)						
H(9)	0.135(9)	0.720(3)	0.494(9)	0.035(7)						
H(10)	0.145(10)	0.625(6)	0.570(7)	0.035(7)						
H(11)	−0.102(9)	0.751(6)	0.171(5)	0.035(7)						
H(12)	−0.042(8)	0.769(6)	0.312(6)	0.035(7)						
H(13)	0.837(8)	0.655(5)	0.913(8)	0.035(7)						
H(14)	0.862(8)	0.572(6)	0.831(9)	0.035(7)						

* Refined occupancy: $Cd_{0.89}Zn_{0.11}$

TABLE 5. Selected interatomic distances (Å) and angles (º) for edwardsite.

Cd(1)–O(4)	2.197(4)	Cd(2)–OH(9)	2.239(5)
H_2O(17)	2.246(4)	OH(14)	2.281(5)
O(8)	2.256(4)	OH(10)	2.288(4)
O(3)	2.279(4)	OH(13)	2.322(5)
H_2O(16)	2.340(5)	OH(12)	2.350(4)
H_2O(15)	2.387(5)	H_2O(18)	2.377(5)
<Cd(1)–O>	2.285	OH(11)	2.378(4)
		<Cd(2)–O>	2.319
Cu(1)–OH(10)	1.950(4)	Cu(2)–OH(9)	1.978(4)
OH(11)	1.959(5)	OH(9)	1.978(4)
OH(9)	1.972(4)	OH(12)	1.981(4)
OH(13)	1.982(4)	OH(12)	1.981(4)
O(2)	2.538(4)	O(5)	2.430(4)
O(5)	2.611(4)	O(5)	2.430(4)
<Cu(1)–O>	2.169	<Cu(2)–O>	2.130
Cu(3)–OH(14)	1.947(4)	Cu(4)–OH(12)	1.955(4)
OH(14)	1.947(4)	OH(11)	1.956(4)
OH(13)	1.982(4)	OH(14)	1.963(4)
OH(13)	1.982(4)	OH(10)	1.984(5)
O(2)	2.538(4)	O(2)	2.363(5)
O(2)	2.538(4)	O(5)	2.838(5)
<Cu(3)–O>	2.156	<Cu(4)–O>	2.176
S(1)–O(1)	1.462(5)	S(2)–O(5)	1.468(5)
O(2)	1.468(5)	O(6)	1.482(5)
O(3)	1.487(5)	O(8)	1.487(5)
O(4)	1.492(5)	O(7)	1.488(4)
<S(1)–O>	1.477	<S(2)–O>	1.481
O(1)–S(1)–O(2)	110.7(3)	O(5)–S(2)–O(6)	110.4(3)
O(1)–S(1)–O(3)	110.5(3)	O(5)–S(2)–O(7)	109.2(3)
O(1)–S(1)–O(4)	109.1(3)	O(5)–S(2)–O(8)	109.3(2)
O(2)–S(1)–O(3)	109.8(3)	O(6)–S(2)–O(7)	109.3(3)
O(2)–S(1)–O(4)	107.2(3)	O(6)–S(2)–O(8)	109.1(3)
O(3)–S(1)–O(4)	109.5(2)	O(7)–S(2)–O(8)	109.6(3)
<O–S(1)–O>	109.47	<O–S(2)–O>	109.48

the Cu and Zn scattering factors, and their similar ionic radii (Shannon, 1976), determination of their distribution on structural sites is difficult to obtain using either X-ray diffraction or the observed bond lengths. Inspection of the bond-length distortion for the Cu octahedra however, suggests that any Zn for Cu substitution is predominantly at the Cu(2) site, with minor Zn at the Cu(1) and Cu(3) sites and no Zn at the Cu(4) site.

The structure contains two symmetrically distinct Cd sites. The Cd(1) site is coordinated by three O^{2-} anions and three H_2O groups in a distorted octahedral arrangement. The <Cd–ϕ> bond length of 2.285 Å (range 2.197(4)–2.387(5) Å) compares well with the average of 2.305 Å [range: 2.169–2.446 Å] for Cd^{2+} in octahedral coordination in Cd oxysalt minerals (Cooper and Hawthorne, 1996, 2000, 2004; Giester *et al.*, 1998; Elliott *et al.*, 2008, 2009). The <Cd–O> distance for full occupancy by Cd, calculated using the ionic radii of Shannon (1976), is 2.307 Å. The octahedral angles range from 81.26 to 108.98º. The refined occupancy suggests that the Cd(1) site is fully occupied by Cd.

TABLE 6. Bond-valence analysis for edwardsite.

	Cd(1)	Cd(2)	Cu(1)	Cu(2)	Cu(3)	Cu(4)	S(1)	S(2)	H(1)	H(2)	H(3)	H(4)	H(5)	H(6)	H(7)	H(8)	H(9)	H(10)	H(11)	H(12)	H(13)	H(14)	Sum excluding H	Sum including H
O(1)							1.55												0.21		0.15		1.55	1.91
O(2)			0.10		0.10↓→ 0.10↓	0.16	1.52																1.88	1.88
O(3)	0.36						1.44					0.10						0.18					1.80	2.08
O(4)	0.45						1.50												0.10			0.12	1.95	2.17
O(5)			0.08 0.1↓	0.13↓→		0.04		1.52															1.77	1.77
O(6)								1.47			0.18				0.16			0.11					1.47	1.92
O(7)								1.45								0.16	0.21			0.15		0.10	1.45	2.07
O(8)	0.39							1.44	0.15														1.83	1.98
OH(9)		0.38	0.45	0.45↓→ 0.45↓					0.85														1.28	2.13
OH(10)		0.34	0.48			0.44				0.89													1.26	2.15
OH(11)		0.25	0.47			0.47					0.82												1.19	2.01
OH(12)		0.29		0.44↓→ 0.44↓		0.47						0.90											1.20	2.10
OH(13)		0.31	0.44		0.44↓→ 0.44↓								0.88										1.19	2.07
OH(14)		0.34			0.49↓→ 0.49↓	0.47								0.89									1.30	2.19
$H_2O(15)$	0.27													0.11	0.84	0.84							0.27	2.06
$H_2O(16)$	0.31												0.12				0.79	0.71					0.31	1.93
$H_2O(17)$	0.40									0.11									0.69	0.85			0.40	2.05
$H_2O(18)$		0.27																			0.85	0.78	0.27	1.90
Sum	2.18	2.18	2.02	2.04	2.06	2.05	6.01	5.88	1.00	1.00	1.00	1.00	1.00	1.00	1.00	1.00	1.00	1.00	1.00	1.00	1.00	1.00		

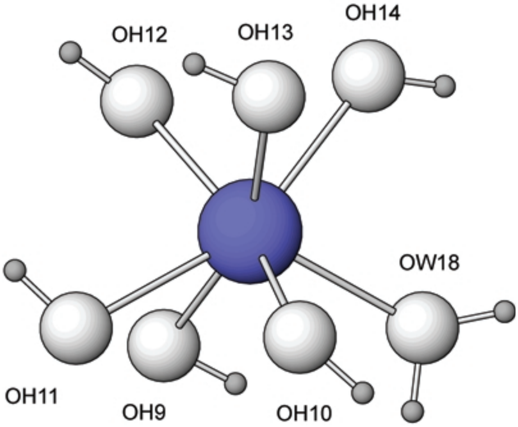

FIG. 4. The coordination environment of the Cd(2) site in edwardsite. The Cd atom is shaded blue, O atoms are shaded pale grey, H atoms are shaded dark grey. All structure drawings were completed using *ATOMS* (Shape Software, 1997).

The Cd(2) site is coordinated by six OH groups and one H_2O group arranged as a diminished square antiprism (Fig. 4). Site-occupancy refinement, using the Cd scattering factor, indicated the presence of one or more lighter atoms, suggesting that some Zn and/or Cu substitutes for Cd. The scattering factors of Cu and Zn are similar however, and refinement of the Cd:Zn ratio resulted in a value of 0.89(9):0.11. The observed <Cd–O> distance of 2.319 Å is compatible with occupancy of the site by either $Cd_{0.88}Zn_{0.12}$ or $Cd_{0.88}Cu_{0.12}$, calculated using the effective ionic radii given by Shannon (1976).

The structure contains two symmetrically distinct S sites, each coordinated by four O^{2-} anions in a tetrahedral arrangement. The <S–O> distances of 1.477 and 1.481 Å for S(1) and S(2) respectively are consistent with the average <S–O> length of 1.473 Å, typical for a sulphate ion (Hawthorne *et al.*, 2000). Tetrahedral bond angles range from 107.2(3) to 110.7(3)º for the $S(1)O_4$ tetrahedron, and from 107.33 to 110.55º for the $S(2)O_4$ tetrahedron. Bond-valence sums for S(1) and S(2) of 6.02 and 5.88 respectively, (Table 6) and site occupancy refinements are in accord with complete occupancy of the sites by S.

Structure connectivity

The structure of edwardsite is based on infinite sheets of composition $[Cu_6Cd_2(SO_4)_4OH_{12}(H_2O)_2]^{4-}$ parallel to (100), which comprise edge-sharing $Cu\phi_6$ (ϕ: O, OH) octahedra and $Cd\phi_7$ (ϕ: OH, H_2O) diminished square antiprisms (Fig. 5). The sheet is a variant of a $[Cu^{2+}\phi_2]_N$ sheet of edge-sharing octahedra that is the basic structural unit of many hydroxy-(hydrated) Cu^{2+} oxysalt minerals (Hawthorne and Schindler, 2000), but with 25% of octahedral sites replaced with a [7]-coordinated Cd site. Sheets are decorated on both sides by corner-sharing (SO_4) tetrahedra, which link to the O(2) and O(5) anions. As with other structures based on brucite-like $[M\phi_2]_N$ sheets of edge-sharing octahedra, three $Cu-\phi_{apical}$ bonds of each constituent octahedron are incident to the coordinating O(2) and O(5) anions in order to satisfy local bond-valence requirements (Hawthorne and Schindler, 2000). Linkage between the sheets is achieved *via* isolated $Cd(1)\phi_6$ octahedra, each of which link to two $S(1)O_4$ tetrahedra and one $S(2)O_4$ tetrahedron by corner sharing (Fig. 6).

H_2O and OH groups and hydrogen bonding

Bond-valence calculations (Table 6) show that there are six OH groups and four H_2O groups in the structure, in accord with the stereochemistry of the H atoms located during the refinement. The six OH groups in the structure are contained within the $[Cu_6Cd_2(SO_4)_4OH_{12}(H_2O)_2]^{4-}$ sheet. Of the four symmetrically distinct H_2O groups, three [$H_2O(15)$, $H_2O(16)$ and $H_2O(17)$] are coordinated to the Cd(1) cation, and $H_2O(18)$ is coordinated to the Cd(2) cation. The crystal-structure refinement indicates that all OH and H_2O groups are fully occupied. Bond lengths and angles for the H bonds are given in Table 7 and the H bond arrangement is shown in Figs 7 and 8. Each of the water molecules $H_2O(17)$, $H_2O(16)$ and $H_2O(15)$ are both providers and acceptors of H bonds, which provide linkage between the sheets and the Cd(1) cation. The $H_2O(15)$ group provides two and the $H_2O(16)$ and $H_2O(17)$ groups each provide three H bonds accepted by the O(1), O(3), O(4), O(6) and O(7) atoms coordinated to S(1) and S(2). Each of the H(2), H(5) and H(6) atoms, bonded to OH groups OH(10), OH(13) and OH(14), provide a single H bond to $H_2O(17)$, $H_2O(16)$ and $H_2O(15)$ respectively. The H(13) atom bonded to $H_2O(18)$ donates a H bond accepted by O(1), and H(14) donates a bifurcated H bond accepted by O(4) and O(7). Hydrogen bonds located within the sheets are provided by H(1), H(3), and H(4) bonded to OH groups OH(9), OH(11), and OH(12) respectively, each donating a single H bond

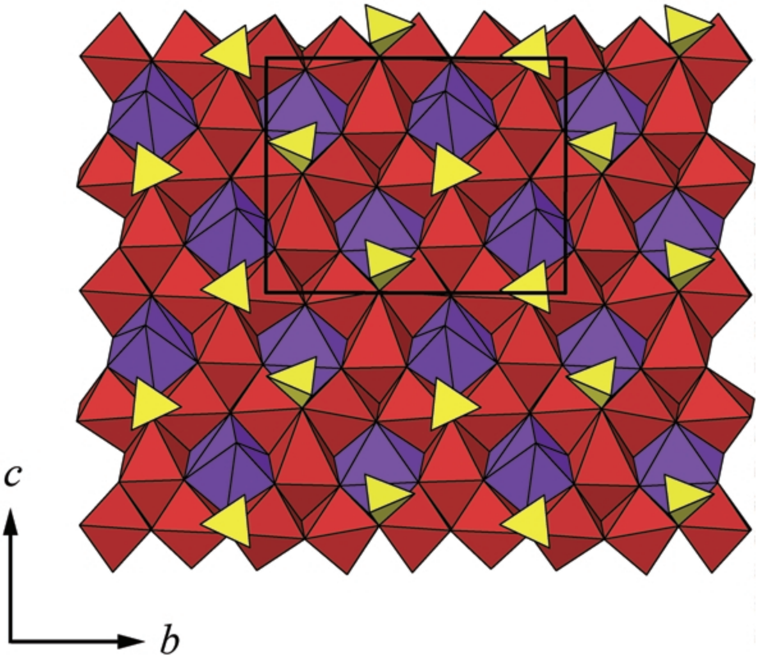

FIG. 5. The crystal structure of edwardsite viewed along [100]; Cuϕ_6 octahedra are red; Cdϕ_7 polyhedra are purple; SO_4 tetrahedra are yellow. The unit cell is outlined.

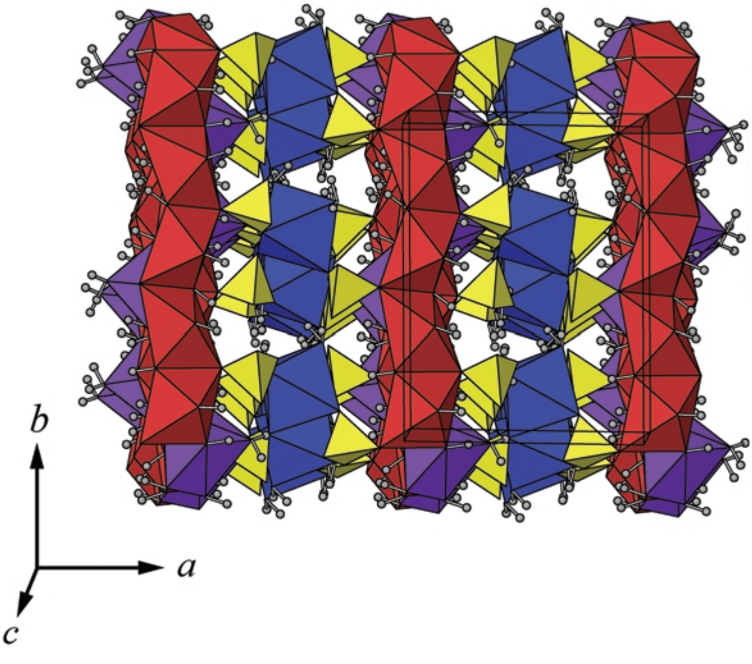

FIG. 6. The crystal structure of edwardsite viewed along a direction close to [001]; Cuϕ_6 octahedra are red; Cdϕ_7 polyhedra are purple; Cdϕ_6 polyhedra are blue; SO_4 tetrahedra are yellow. The unit cell is outlined.

TABLE 7. Details of hydrogen bonding in edwardsite (Å, º).

D–H···*A*	*D*–H	H···*A*	*D*···*A*	∠*D*–H···*A*
OH(9)–H(1)···O(8)$^{\mathrm{i}}$	0.93(5)	2.23(8)	2.865(6)	125(8)
OH(10)–H(2)···$\mathrm{H_2O}$(17)$^{\mathrm{ii}}$	0.93(5)	2.11(6)	2.986(6)	157(8)
OH(11)–H(3)···O(6)$^{\mathrm{iii}}$	0.94(5)	1.92(5)	2.846(6)	173(9)
OH(12)–H(4)···O(3)	0.96(5)	2.27(7)	3.097(6)	143(8)
OH(13)–H(5)···$\mathrm{H_2O}$(16)	0.92(5)	2.02(5)	2.940(6)	176(8)
OH(14)–H(6)···$\mathrm{H_2O}$(15)	0.93(5)	2.09(6)	2.984(7)	160(9)
$\mathrm{H_2O}$(15)–H(7)···O(6)$^{\mathrm{iv}}$	0.94(5)	1.91(5)	2.803(6)	157(7)
$\mathrm{H_2O}$(15)–H(8)···O(7)$^{\mathrm{v}}$	0.94(5)	2.12(7)	2.910(7)	141(7)
$\mathrm{H_2O}$(16)–H(9)···O(7)$^{\mathrm{iv}}$	0.94(3)	1.78(4)	2.687(6)	163(8)
$\mathrm{H_2O}$(16)–H(10)···O(6)	0.92(5)	2.21(7)	2.973(7)	139(7)
$\mathrm{H_2O}$(16)–H(10)···O(3)	0.92(5)	2.33(7)	2.843(6)	115(6)
$\mathrm{H_2O}$(17)–H(11)···O(1)$^{\mathrm{vi}}$	0.97(5)	1.73(5)	2.679(7)	166(7)
$\mathrm{H_2O}$(17)–H(11)···O(4)$^{\mathrm{vi}}$	0.97(5)	2.38(8)	3.000(6)	122(6)
$\mathrm{H_2O}$(17)–H(12)···O(7)$^{\mathrm{iv}}$	0.97(5)	1.90(5)	2.860(7)	170(9)
$\mathrm{H_2O}$(18)–H(13)···O(1)$^{\mathrm{vii}}$	0.94(5)	1.95(5)	2.869(7)	166(7)
$\mathrm{H_2O}$(18)–H(14)···O(4)$^{\mathrm{viii}}$	0.93(5)	2.21(8)	2.933(7)	134(8)
$\mathrm{H_2O}$(18)–H(14)···O(7)$^{\mathrm{ix}}$	0.93(5)	2.57(8)	3.060(7)	114(6)

Symmetry codes: (i) $-x+1, -y+1, -z+2$; (ii) $x+1, y, z+1$; (iii) $-x+1, y-1/2, -z+3/2$; (iv) $x, -y+3/2, z-1/2$; (v) $x, y, z-1$; (vi) $-x, y+1/2, -z+1/2$; (vii) $-x+1, y+1/2, -z+3/2$; (viii) $-x+1, -y+1, -z+1$; (ix) $x+1, y, z$.

accepted by the O(8), O(6) and O(3) atoms. All H bonds involve O···O distances from 2.65(2) to 3.05(4) Å so would represent medium-strong to weak links.

Structural relations

The sheet in the edwardsite structure is a variant of an $[M\phi_2]_N$ sheet of edge-sharing octahedra (brucite-type sheets), a common stoichiometry for

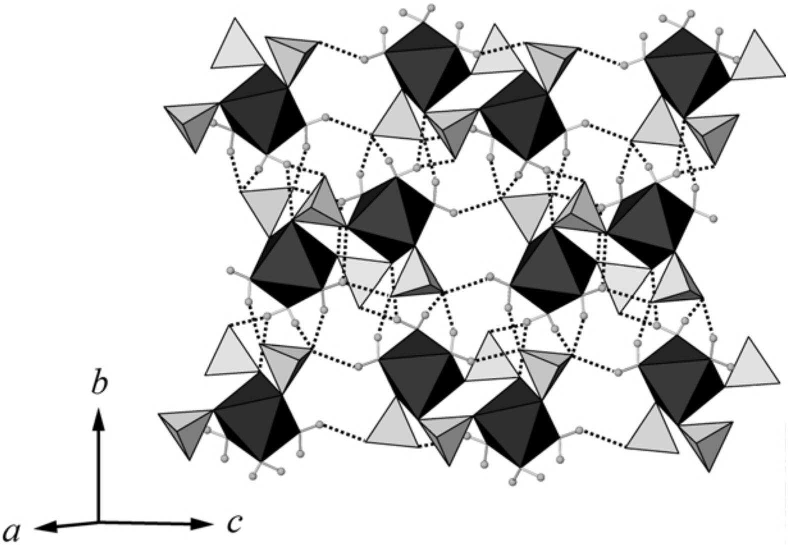

FIG. 7. The crystal structure of edwardsite viewed along [100]; $\mathrm{Cd\phi_6}$ octahedra are dark grey; $\mathrm{SO_4}$ tetrahedra are pale grey; H atoms are small grey spheres. Hydrogen bonds are shown as dotted lines.

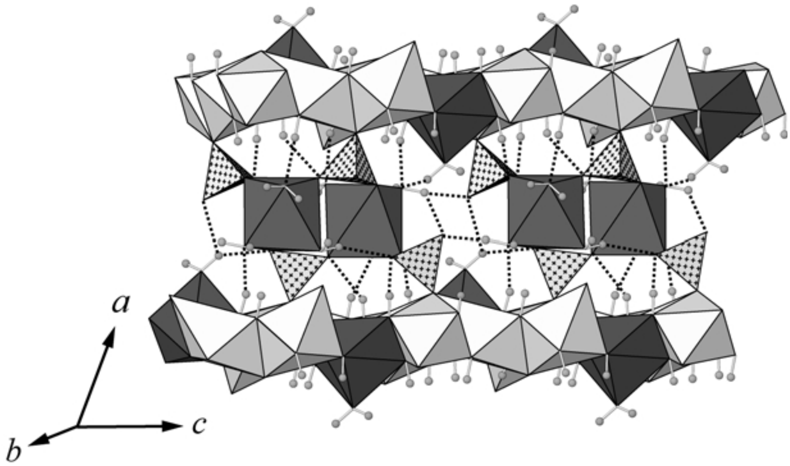

FIG. 8. The crystal structure of edwardsite viewed along a direction close to [101]; Cuϕ_6 octahedra are white; Cdϕ_6 octahedra are dark grey; Cdϕ_7 polyhedra are dark grey; SO_4 tetrahedra are cross-shaded; H atoms are small grey spheres. Hydrogen bonds are indicated by dotted lines.

polyhedral sheets in mineral structures. Sheets in which *M* = (Cu^{2+}, Zn) are the basis for the structures of many hydroxy-(hydrated) Cu^{2+} oxysalt minerals, in particular Cu^{2+} and Zn sulphates (Eby and Hawthorne, 1993; Hawthorne and Schindler, 2000). Sheets are either one-side-decorated by SO_4 tetrahedra [e.g. langite, $Cu_4^{2+}(SO_4)(OH)_6{\cdot}2H_2O$ (Gentsch and Weber, 1984), posnjakite, $Cu_4SO_4(OH)_6{\cdot}H_2O$ (Mellini and Merlino, 1979), wroewolfeite $Cu_2(SO_4)(OH)_6{\cdot}2H_2O$ (Hawthorne and Groat, 1985), spangolite, $Cu_6Al(SO_4)Cl(OH)_{12}{\cdot}3H_2O$ (Merlino *et al.*, 1992; Hawthorne *et al.*, 1993), montetrisaite, $Cu_6(SO_4)(OH)_{10}{\cdot}2H_2O$ (Orlandi and Bonaccorsi, 2009)], or two-side-decorated by SO_4 tetrahedra [e.g. niedermayrite, $Cu_4Cd(SO_4)_2(OH)_6{\cdot}4H_2O$ (Giester *et al.*, 1998), christelite, $Zn_3Cu_2(SO_4)_2(OH)_6{\cdot}4H_2O$ (Adiwidjaja *et al.*, 1996), lautenthalite, $PbCu_4(SO_4)_2(OH)_6{\cdot}3H_2O$ (Medenbach and Gebert, 1993), ktenasite, $Zn_2(Cu,Zn)_8(OH)_{12}(SO_4)_4{\cdot}12H_2O$ (Mellini and Merlino, 1978), serpierite, $Ca(Cu,Zn)_4(SO_4)_2(OH)_6{\cdot}3H_2O$ (Sabelli and Zanazzi, 1968), devilline, $Ca(Cu,Zn)_4(OH)_6(SO_4)_2{\cdot}3H_2O$ (Sabelli and Zanazzi, 1972), schulenbergite $(Cu,Zn)_7(OH)_{10}(SO_4)_2{\cdot}2H_2O$ (Mumme *et al.*, 1994)]. Linkage between adjacent sheets is provided *via* H bonds only in the structures of posnjakite, langite, wroewolfeite, spangolite, schulenbergite and montetrisaite. Hydrogen bonds are either between OH groups coordinated to the sheet cations and O atoms of SO_4 tetrahedra (posnjakite, langite and wroewolfeite), or are transmitted between sheets *via* interstitial H_2O groups (montetrisaite), or both (spangolite, schulenbergite). Linkage between adjacent sheets can also be provided *via* isolated $M\phi_n$ (*M*: Ca, Zn, Cd, Pb; ϕ: H_2O) polyhedra, which either link to the sheets *via* corner-sharing SO_4 tetrahedra (e.g. niedermayrite, christelite, serpierite, devilline, lautenthalite), or link to the sheets by H bonding only between the $M(H_2O)_6$ polyhedra and O atoms of the SO_4 tetrahedra (e.g. ktenasite).

A variant of the $[Cu^{2+}\phi_2]_N$ sheet of edge-sharing octahedra that has 25% of octahedral sites replaced by a regular Cdϕ_6 octahedron, with six equal Cd–O lengths of 2.27 Å, is found in the structure of the synthetic compound $CdCu_3(OH)_6(NO_3)_2{\cdot}H_2O$ (Oswald, 1969). The sheet, which has composition $[Cu_4^{2+}\ X_2\ \phi_6]$, is homeomorphic to graph 3c of Hawthorne and Schindler (2000), in which a central ($M\phi_6$) octahedron sits inside the six-membered ring formed by apical Cu^{2+}–ϕ bonds. Homeomorphisms also occur in the sheets of langite, posnjakite and claringbullite. In langite and posnjakite the central octahedrally coordinated position is occupied by a [4 + 2]-distorted ($Cu^{2+}\phi_6$) octahedron. In claringbullite, $Cu_4^{2+}Cl[(OH)Cl](OH)_6$, (Burns *et al.*, 1995) this octahedral position is vacant. In edwardsite, this position is occupied by the $Cd^{2+}\phi_7$ diminished square antiprism.

Acknowledgements

The specimen containing edwardsite was kindly provided by Steve Taylor. We thank Angus Netting and John Terlet of Adelaide Microscopy, The University of Adelaide for their assistance with the microprobe analysis. Gerald Geister and Uwe Kolitsch are thanked for assistance with the initial attempts to collect single crystal X-ray data. We are grateful to Hayley Brown and Paul Pigou for assistance with collection of the infrared spectrum and Ruth Plathe for help during synchrotron data collection. The manuscript was improved by comments from reviewers Anthony Kampf and Daniel Atencio and from crystal structures editor Fernando Camara. P.E. wishes to acknowledge the financial support of an Australian Postgraduate Award.

References

Adiwidjaja, G., Friese, K., Klaska, K.-H. and Schlüter, J. (1996) The crystal structure of christelite $Zn_3Cu_2(SO_4)_2(OH)_6\cdot4H_2O$. *Zeitschrift für Kristallographie*, **211**, 518–521.

Birch, W.D. (1999) The Minerals. Pp. 88–356 in: *Minerals of Broken Hill* (W.D. Birch, editor) Broken Hill Council, Broken Hill, Australia.

Both, R.A. (1973) Minor element geochemistry of sulphide minerals in the Broken Hill lode (N.S.W.) in relation to the origin of the ore. *Mineralium Deposita*, **8**, 349–369.

Bregeault, J.M. and Herpin, P. (1970) Crystal structure of $CdSO_4.H_2O$. *Bulletin. Société Français de Minèralogie et de Cristallographie*, **93**, 37–42. (in French).

Brese, N.E. and O'Keeffe, M. (1991) Bond–valence parameters for solids. *Acta Crystallographica B*, **47**, 192–197.

Brown, I.D. (1996) VALENCE: a program for calculating bond valences. *Journal of Applied Crystallography*, **29**, 479–480.

Brown, I.D. and Altermatt, D. (1985) Bond–valence parameters obtained from a systematic analysis of the inorganic crystal structure database. *Acta Crystallographica B*, **41**, 244–247.

Burns, P.C. and Hawthorne, F.C. (1996) Static and dynamic Jahn–Teller effects in Cu^{2+} oxysalts. *The Canadian Mineralogist*, **34**, 1089–1105.

Burns, P.C., Cooper, M.A. and Hawthorne, F.C. (1995) Claringbullite: a Cu^{2+} oxysalt with Cu^{2+} in trigonal-prismatic coordination. *The Canadian Mineralogist*, **33**, 633–639.

Cooper, M.A. and Hawthorne, F.C. (1996) The crystal structure of keyite, $Cu_3(Zn,Cu)_4Cd_2(AsO_4)_6(H_2O)_2$, an oxysalt mineral with essential cadmium. *The Canadian Mineralogist*, **34**, 623–630.

Cooper, M.A. and Hawthorne, F.C. (2000) Highly undersaturated anions in the crystal structure of andyrobertsite–calcio-andyrobertsite, a doubly acid arsenate of the form $K(Cd,Ca)[Cu_5^{2+}(AsO_4)_4\{As(OH)_2O_2\}](H_2O)_2$. *The Canadian Mineralogist*, **38**, 817–830.

Cooper, M.A. and Hawthorne, F.C. (2004) The crystal structure of goldquarryite, $(Cu^{2+},\square)(Cd,Ca)_2Al_3(PO_4)_4F_2(H_2O)_{10}\{(H_2O),F\}_2$, a secondary phosphate from the Gold Quarry mine, Eureka County, Nevada, U.S.A. *The Canadian Mineralogist*, **42**, 753–761.

Eby, R.K. and Hawthorne, F.C. (1993) Structural relationships in copper oxysalt minerals. I. Structural hierarchy. *Acta Crystallographica B*, **49**, 28–56.

Edwards, A.B. (1955) Cadmium in the Broken Hill lode. *Proceedngs of the Australasian Institute of Mining and Mellallurgy*, **176**, 71–96.

Elliott, P., Brugger, J., Pring, A., Cole, M.L., Willis, A.C. and Kolitsch, U. (2008) Birchite, a new mineral from Broken Hill, New South Wales, Australia: description and structure refinement. *American Mineralogist*, **93**, 910–917.

Elliott, P., Turner, P., Jensen, P., Kolitsch, U. and Pring, A. (2009) Description and crystal structure of nyholmite, a new mineral related to hureaulite, from Broken Hill, New South Wales, Australia, *Mineralogical Magazine*, **73**, 723–735.

Giester, G., Rieck, B. and Brandstätter, F. (1998) Niedermayrite, $Cu_4Cd(SO_4)_2(OH)_6\cdot4H_2O$, a new mineral from the Lavrion District, Greece. *Mineralogy and Petrology*, **63**, 9–34.

Giester, G., Kolitsch, U., Leverett, P., Turner, P. and Williams, P.A. (2007) The crystal structures of lavendulan, sampleite, and a new polymorph of sampleite. *European Journal of Mineralogy*, **19**, 75–93.

Gentsch, M. and Weber, K. (1984) Structure of langite, $Cu_4[(OH)_6(SO_4)]\cdot2(H_2O)$. *Acta Crystallographica C*, **40**, 1309–1311.

Hawthorne, F.C. and Groat, L.A. (1985) The crystal structure of wroewolfeite, a mineral with $[Cu_4(OH)_6(SO_4)(H_2O)]$ sheets. *American Mineralogist*, **70**, 1050–1055.

Hawthorne, F.C. and Schindler, M.S. (2000) Topological enumeration of decorated $[Cu^{2+}\phi_2]_N$ sheets in hydroxy-hydrated copper-oxysalt minerals. *The Canadian Mineralogist*, **38**, 751–761.

Hawthorne, F.C., Kimata, M. and Eby, R.K. (1993) The crystal structure of spangolite, a complex copper sulfate sheet mineral. *American Mineralogist*, **78**, 649–652.

Hawthorne, F.C., Krivovichev, S.V. and Burns, P.C. (2000) The crystal chemistry of sulfate minerals. Pp. 1–112 in: *Sulfate Minerals: Crystallography, Geochemistry, and Environmental Significance*. (C.N. Alpers, J.L. Jambor and D.K. Nordstrom, editors). Reviews in Mineralogy, **40**. Mineralogical Society of America, Chantilly, Virginia, USA.

Hunter, B.A. (1998) Rietica - A Visual Rietveld Program. *Commission on Powder Diffraction Newsletter*, **20**, 21.

Jahn, H.A. and Teller, E. (1937) Stability of polyatomic molecules in degenerate electronic states. *Proceedings of the Royal Society, Series A*, **161**, 220–236.

Le Bail, A., Duroy, H. and Fourquet, J.L. (1988) Ab-initio structure determination of $LiSbWO_6$ by X-ray powder diffraction. *Materials Research Bulletin*, **23**, 447–452.

Libowitzky, E. (1999) Correlation of O-H stretching frequencies and O–H···O hydrogen bond lengths in minerals. *Monatshefte für Chemie*, **130**, 1047–1059.

Medenbach, O. and Gebert, W. (1993) Lautenthalite, $PbCu_4[(OH)_6|(SO_4)_2]{\cdot}3H_2O$, the Pb analogue of devillite – a new mineral from the Harz mountains, Germany. *Neues Jahrbuch fur Mineralogie Monatshefte*, 401–407.

Mellini, M. and Merlino, S. (1978) Ktenasite, another mineral with $[(Cu,Zn)_2(OH)_3O]^-$ octahedral sheets. *Zeitschrift für Kristallographie*, **147**, 129–140.

Mellini, M. and Merlino, S. (1979) Posnjakite: $[Cu_4(OH)_6(H_2O)O]$ octahedral sheets in its structure. *Zeitschrift für Kristallographie*, **149**, 249–257.

Merlino, S., Pasero, M., Sabelli, C. and Trosti-Ferroni, R. (1992) Crystal structure refinements of spangolite, a hydrated basic sulphate of copper and aluminum, from three different occurrences. *Neues Jahrbuch für Mineralogie Monatshefte*, 349–357.

Mumme, W.G., Sarp, H. and Chiappero. P.J. (1994) A note on the crystal structure of schulenbergite, *Archives des Sciences, Genève*, **47**, 117–124.

Orlandi, P. and Bonaccorsi, E. (2009) Montetrisaite, a new hydroxy-hydrated copper sulphate from Italy. *The Canadian Mineralogist*, **47**, 143–151.

Oswald, H.R. (1969) Kristallstruktur von Cadmium-Kupfer-Hydroxidnitrat, $CdCu_3(OH)_6(NO_3)_2{\cdot}H_2O$. *Helvetica Chimica Acta*, **52**, 2369–2380.

Plimer, I.R. (1984) The mineralogical history of the Broken Hill Lode, NSW. *Australian Journal of Earth Sciences*, **31**, 379–402.

Pouchou, J.L. and Pichoir, F. (1985) 'PAP' $\phi(\rho Z)$ procedure for improved quantitative microanalysis. Pp. 104–106 in: *Microbeam Analysis*, (J.T. Armstrong, editor). San Francisco Press, San Francisco, California, USA.

Sabelli, C. and Zanazzi, P.F. (1968) The crystal structure of serpierite. *Acta Crystallographica B*, **24**, 1214–1221.

Sabelli, C. and Zanazzi, P.F. (1972) The crystal structure of devillite. *Acta Crystallographica B*, **28**, 1182–1189.

Sejkora, J. and Kotrlý, M. (1998) A new cadmium sulfate natural phase from Radvanice near Trutnov (Czech Republic). *Bulletin of the Czech Geological Survey*, **73**, 321–326.

Shannon, R.D. (1976) Revised effective ionic radii and systematic studies of interatomic distances in halides and chalcogenides. *Acta Crystallographica A*, **32**, 751–767.

Shape Software (1997) *ATOMS for Windows and Macintosh V 4.0*, Kingsport, Tennessee, USA.

Shape Software (2004) *SHAPE for Windows and Macintosh V 7.1.2*, Kingsport, Tennessee, USA.

Sheldrick, G.M. (1997*a*) *SHELXS-97, a Program for the Solution of Crystal Structures*. University of Göttingen, Göttingen, Germany.

Sheldrick, G.M. (1997*b*) *SHELXL-97, a Program for Crystal Structure Refinement*. University of Göttingen, Göttingen, Germany.

Shepard, C.U. (1837) Description of Edwardsite, a New Mineral. *American Journal of Science*, **32**, 162–166.

Shepard, C.U. (1840) On the identity of edwardsite with monazite (mingite) and on the Composition of the Missouri meteorite. *American Journal of Science*, **39**, 249–255.

Stevens, B.P.J. (1998) The origins of the Broken Hill rock types and their relevance to the mineralisation. Pp. 109–114 in: *Abstracts from Broken Hill Exploration Initiative annual meeting, 1998.* Australian Geological Survey Organisation Record 1998/25.

Willis, I.L., Brown, R.E., Stroud, W.J. and Stevens, B.P.J. (1983) The Early Proterozoic Willyama Supergroup: Stratigraphic sub-division and interpretation of high to low grade metamorphic rocks in the Broken Hill Block, N.S.W. *Journal of the Geological Society of Australia*, **30**, 195–224.

Wilson, A.I.C., editor. (1992) *International Tables for Crystallography, vol. C*. Kluwer Academic, Dordrecht, The Netherlands, 883pp.

Yvon, K., Jeitschko, W. and Parthé, E. (1977) LAZY PULVERIX, a computer program, for calculating X-ray and neutron diffraction powder patterns. *Journal of Applied Crystallography*, **10**, 73–74.